ELSEVIER

www.elsevier.nl/locate/jelechem

Journal of Electroanalytical Chemistry 468 (1999) 170–179

JOURNAL OF ELECTROANALYTICAL CHEMISTRY

Formation of a nickel hydroxide monolayer on Au through a self-assembled monolayer of 5,5′-dithiobis(2-nitrobenzoic acid): voltammetric, SERS and XPS investigations of the modified electrodes

Sheela Berchmans [a], V. Yegnaraman [a,*], N. Sandhyarani [b], K.V.G.K. Murty [b], T. Pradeep [b]

[a] *Central Electrochemical Research Institute, Karaikudi-630 006, Tamilnadu, India*
[b] *Department of Chemistry and Regional Sophisticated Instrumentation Centre, Indian Institute of Technology, Chennai 600 036, India*

Received 9 July 1998; received in revised form 17 March 1999; accepted 9 April 1999

Abstract

The formation of self-assembled monolayers (SAM) of 5,5′-dithiobis (2-nitrobenzoic acid), DNBA on gold has enabled further derivatization of the electrode surface with functional moieties anchored to the surface bound molecules. A SAM of DNBA was formed on the Au surface. Nickel ions tethered to the SAM-covered Au surface, were subsequently derivatized electrochemically to yield nickel hydroxide overlayers, thereby showing the possibility of preparing ultra-thin films of metal oxides through solution chemistry. The nickel hydroxide surface coverage obtained on bare and SAM-covered electrodes was estimated from voltammetric peaks and it varied from one monolayer to about 300 monolayers. The formation of a monolayer of nickel hydroxide has been achieved for the first time by electrochemical modification. Further, the modified electrodes were subjected to SERS and XPS studies to understand their surface characteristics. Modified electrodes provide a catalytic pathway involving nickel hydroxide for the electro-oxidation of glucose in alkaline solutions.

Keywords: Self-assembly; Surface modification; Voltammetry; SERS; XPS

1. Introduction

Functionalisation of electrode surfaces with metal oxide (MO) overlayers [1] has been an active field of research in view of its applications to different areas such as electrocatalysis [2–4] and electrochromism [5–7]. Electrochemical modification offers an elegant approach for achieving such MO overlayers on electrode surfaces [8]. However, in this procedure, the control of film growth at the monolayer level is very difficult. Of late, self-assembled monolayer (SAM) modification with organo-sulfur compounds having suitable functional groups has facilitated the immobilisation of relatively thin MO overlayers on the electrode surface [9]. The terminal functional group of the SAM can be advantageously used to tether metal ions [10–13]. This property of SAMs anchored on an electrode surface can be exploited for the formation of MO monolayers.

The choice of the '$Ni(OH)_2 \leftrightarrow NiOOH$' system for incorporation as overlayers, in this study, arose from the reported ability for chelating Ni ions to carboxyl-terminated thiols [12]. Besides, the above redox system possesses excellent reversibility and has been employed extensively and successfully in many application areas like electrochromism [5–7], batteries [14,15] and electroanalysis [2]. The electron transfer kinetics in $Ni(OH)_2$ films have been investigated and are found to depend on factors [3,4] like (a) the electron transfer rate at the substrate | nickel hydroxide interface; (b) the rate of charge transport through nickel hydroxide/oxyhydroxide film and (c) the slow electron hopping through the nickel based film.

* Corresponding author. Tel.: +91-4565-22368 ext. 225; fax: +91-4565-37779/37713.
E-mail address: eeb@cscecri.ren.nic.in (V. Yegnaraman)

0022-0728/99/$ - see front matter
PII: S0022-0728(99)00163-1

In the present investigations, 5,5′-dithiobis(2-nitrobenzoic acid) (DNBA) has been chosen to form SAMs on gold. DNBA, studied here for the first time in the formation of a SAM and subsequent modification, is an aromatic disulfide with two –COOH groups. The utility of the terminal –COOH groups in further chemical modification has already been shown by using mercaptopropionic acid [16,17]. A monolayer of DNBA is formed on Au (designated as Au | DNBA) and it is further modified in the solution phase to yield a monolayer of nickel oxide as an overlayer. The redox characteristics of the modified electrode, denoted as Au | DNBA | $Ni(OH)_2$ (ml) and its catalytic influence on glucose electro-oxidation have been investigated. Moreover, the Au | DNBA electrode with and without $Ni(OH)_2$ modification is subject to SERS and XPS studies. The results are described in this article.

2. Experimental

2.1. Electrodes and chemicals

A gold disk of area 0.024 cm^2 (BAS, USA) was used as the working electrode. A Pt foil and a 1 M KCl calomel electrode (MCE) served as the counter and reference electrodes. All potential values in this study are referred to MCE. The Analar grade sample of DNBA (Aldrich, USA) was used without further purification. Other reagents were also of Analar grade and triply distilled water was used for preparing solutions. The Au | DNBA electrode was prepared by immersing a Au electrode in an ethanol solution of DNBA (4 mM) overnight. Prior to immersion, the electrode was polished, degreased and sonicated in water. After immersion, the electrode was rinsed thoroughly with ethanol, air-dried and stored.

2.2. Incorporation of $Ni(OH)_2$ overlayer on an Au | DNBA electrode

The incorporation of a monolayer of $Ni(OH)_2$ on Au | DNBA was achieved as follows. The Au | DNBA electrode prepared from a 4 mM DNBA solution by the procedure described earlier, was immersed for 4 h in 1 M KCl containing 2.5 mM $NiSO_4$. Afterwards the electrode was washed thoroughly in water and then cycled between 0 and 1.0 V at 20 mV s^{-1} in a 0.5 M KCl solution containing 0.25 M HCl + 0.5 mM $K_3[Fe(CN)_6]$. After seven cycles, the electrode was subjected to cycling between 0 and 500 mV at 10 mV s^{-1} in 1 M KOH solution until saturation in film growth was attained. By the above treatments, the nickel hexacyanoferrate (NiHCF) formed in the first stage was derivatized to $Ni(OH)_2$ by cycling in alkali solution during the second stage. It was found that the growth of $Ni(OH)_2$ film attained saturation within two to three cycles. This electrode has been denoted as Au | DNBA | $Ni(OH)_2$(ml).

Also, $Ni(OH)_2$ modification was achieved on Au | DNBA by a standard procedure developed earlier in our laboratory [18,19] and also adapted elsewhere [20]. Briefly, the Au | DNBA electrode was cycled between 0 and 1.0 V at 1 V s^{-1} in 0.5 M KCl solution containing 0.25 M HCl, 0.5 mM $K_3[Fe(CN)_6]$ and 0.5 mM $NiSO_4$ for 30 min. Subsequently, the electrode was subjected to cycling between 0 and 500 mV at 10 mV s^{-1}, in 1 M KOH until saturation in film growth was attained. For comparison, a Au electrode covered directly with $Ni(OH)_2$ film, obtained from seven cycles, was also included in the studies. This electrode was formed employing the bare gold electrode (without SAM coverage) and effecting the modification as above [18,19]. These modified electrodes are referred to as Au | DNBA | $Ni(OH)_2$ and Au | $Ni(OH)_2$, respectively.

2.3. Voltammetric measurements

Cyclic voltammetric (CV) investigations were performed using a Wenking (Model POS 73) Potentioscan and a Rikadenki (Model RW 201T) X–Y recorder.

2.4. Spectral measurements

Further, the Au | DNBA electrode was subjected to SERS and XPS analysis to understand the characteristics of the adsorbed DNBA molecules. For this, electrochemically roughened gold foil was used as the substrate. For carrying out UV diffuse reflectance studies, Au-coated glass electrodes of 1 cm^2 area were used and the surface modification was effected in the same way as described above. For UV diffuse reflectance studies, a Hitachi (Model U300) UV-vis spectrophotometer was used. Raman measurements were carried out with a Bruker IFS 66V FT-IR spectrometer with a FRA 106 FT-Raman attachment. An Nd-YAG laser (1064 nm) was used for primary excitation. XPS measurements were conducted with a VG ESCALAB Mk II spectrometer with unmonochromatised Mg K_α radiation. Samples were inserted into the UHV chamber soon after they were prepared. Measurements were done under a pressure of 10^{-9} Torr. In order to minimize the X-ray beam induced damage, the X-ray flux was kept low (electron power, 70 W). For the $Ni(OH)_2$ modified samples, mild etching of surface contaminants was necessary to obtain the Ni, C and S signals. Due to significant attenuation of the photoelectron signals

caused by the overlayer, the spectral quality of the modified electrodes is marginal. Further, it may be recalled that all the above elements are present only in monolayer quantities and signal loss due to the overlayer attenuation was substantial.

3. Results and discussion

3.1. Redox behaviour of ferro/ferricyanide at Au | DNBA electrode

Fig. 1 depicts the CV response at 20 mV s^{-1} of $K_4Fe(CN)_6$ (1.66 mM) on Au and Au | DNBA electrodes. It can be seen that ΔE_p, the difference between the anodic ($E_{p,a}$) and the cathodic ($E_{p,c}$) peak potentials for the redox couple, increases and the peak currents decrease as a result of introduction of the DNBA SAM on the electrode surface. Heterogeneous electron transfer rate constants (k_h) were calculated by the Nicholson method [21] using ΔE_p values and the corresponding ψ values from the literature. The values of 3.9×10^{-2} and 2.7×10^{-3} cm s^{-1} for Au and Au | DNBA electrodes, respectively, show that the electron transfer rate is decreased nearly 10-fold due to the presence of the SAM on the electrode surface. The decrease in electron transfer rate at the Au | DNBA electrode arises from the repulsive electrostatic interactions [22] between the $Fe(CN)_6^{3-/4-}$ species and the $-COO^-$ ions of the DNBA molecules self-assembled on the electrode surface. The DNBA molecules will remain ionized in 1 M KCl solution, (background electrolyte), since its pK_a value would be less than 3.41 which is the pK_a value for p-nitrobenzoic acid [23].

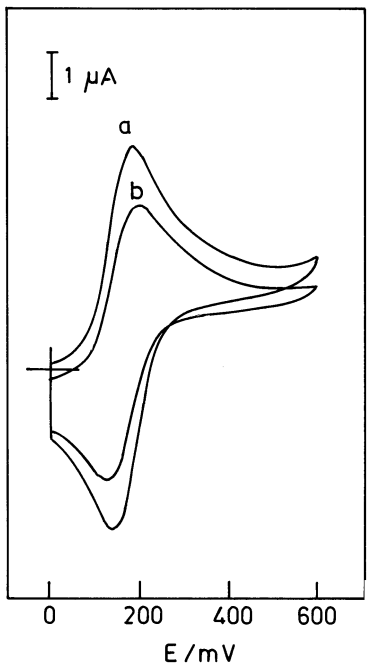

Fig. 1. CV response of $K_4Fe(CN)_6$ (1.66 mM) in 1 M KCl at (a) bare Au and (b) Au | DNBA electrodes. Scan rate: 20 mV s^{-1}.

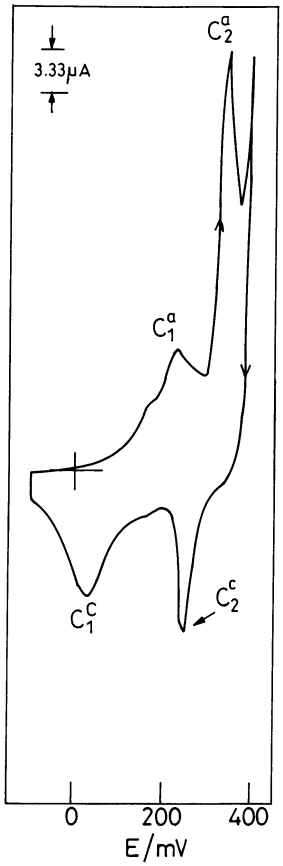

Fig. 2. CV response of Au | $Ni(OH)_2$ electrode in 1 M KOH at 20 mV s^{-1}.

3.2. Redox behaviour of $Ni(OH)_2$-modified electrodes

Fig. 2 describes the CV features of the Au | $Ni(OH)_2$ electrode in 1 M KOH at 20 mV s^{-1}. A pair of anodic (c_2^a) and cathodic (c_2^c) peaks are observed at 345 and 245 mV respectively, yielding a ΔE_p value of 100 mV. The peak-width at half maximum (E_{fwhm}) is noted as 50 and 30 mV for the anodic and cathodic peaks respectively. Another pair of anodic and cathodic peaks (c_1^a and c_1^c) are noticed at 220 and 20 mV, respectively. These peaks could be assigned to the formation and reduction of Au oxide on bare gold in the background electrolyte [24].

Fig. 3(a) describes the CV behaviour of Au | DNBA | $Ni(OH)_2$(ml) recorded at 20 mV s^{-1} in 1 M KOH. The anodic peak occurs at 0.350 V while the cathodic peak is at 0.270 V with a ΔE_p value of 80 mV. The E_{fwhm} values are estimated to be 45 and 35 mV for the anodic and cathodic peaks respectively. Fig. 3(b) shows the voltammetric features of the Au | DNBA | $Ni(OH)_2$ electrode recorded at 20 mV s^{-1} in 1 M KOH. The anodic peak occurs at 0.340 V and the cathodic peak at 0.200

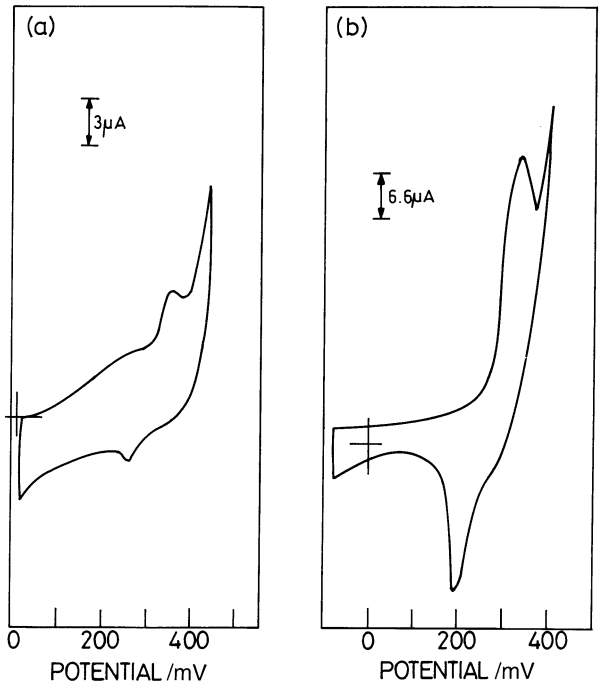

Fig. 3. Redox behaviour of (a) Au | DNBA | $Ni(OH)_2$(ml) and (b) Au | DNBA | $Ni(OH)_2$ electrodes at 20 mV s^{-1} in 1 M KOH.

V, yielding values of 70, 50 and 140 mV for E^{a}_{fwhm}, E^{c}_{fwhm} and $\Delta E_{p,}$ respectively. It may be noted that the above peak potentials are in good agreement with the peak potentials observed for the oxidation of $Ni(OH)_2$ and its subsequent reduction on bare Au (cf. Fig. 2) and also with those reported earlier [25,26], thereby showing that the modification has resulted in the incorporation of $Ni(OH)_2$ species on the electrode surface.

Further, the presence of $Ni(OH)_2$ overlayers on the above-modified electrodes derives additional support from UV diffuse reflectance studies. Fig. 4 depicts the UV spectra obtained at the Au | DNBA | $Ni(OH)_2$ electrode. The broad band seen between 300 and 500 nm is in very good agreement with that of surface-immobilized $Ni(OH)_2$ species observed earlier [6]. The fact that no such band was observed at the Au | DNBA electrode confirms the presence of $Ni(OH)_2$ overlayers on the modified electrodes.

3.3. Voltammetric characteristics of $Ni(OH)_2$ modified electrodes

Table 1 gives the values of surface coverage by $Ni(OH)_2$ obtained by integration of the charge under the anodic peaks of CVs recorded at 20 mV s^{-1} in 1 M KOH at different modified electrodes described above. Based on the fact that one monolayer coverage of $Ni(OH)_2$ corresponds to 1.06×10^{-9} mol cm^{-2} [27], the present investigations show that on Au | DNBA | $Ni(OH)_2$(ml), the coverage corresponds to one monolayer while on Au | DNBA | $Ni(OH)_2$, a saturation coverage of about 30 monolayers results. On the other hand, on bare Au when modification was restricted to seven potential cycles [same as the number of cycles employed for preparing Au | DNBA | $Ni(OH)_2$(ml)], $Ni(OH)_2$ film is about nine monolayers thick while prolonged cycling has been shown to yield films thicker than 100 monolayers [27].

Surface processes [28] are characterized typically by $\Delta E_p \rightarrow 0$. On the other hand, surface-confined redox couples with slow charge transfer kinetics exhibit ΔE_p values not approaching zero even at very low scan

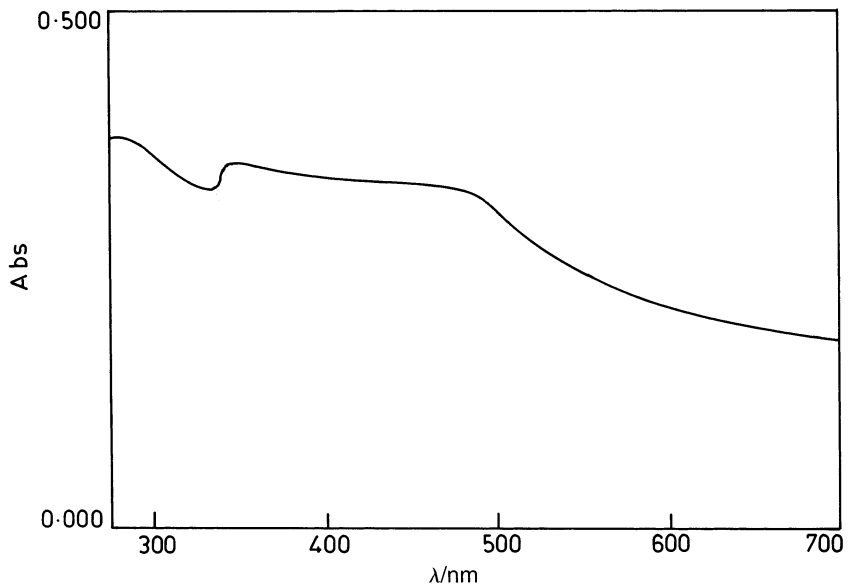

Fig. 4. UV diffuse reflectance spectrum for the Au | DNBA | $Ni(OH)_2$ electrode.

Table 1
Voltammetric characteristics and $Ni(OH)_2$ coverage at the modified electrodes [a]

Property	Au | $Ni(OH)_2$ (seven cycles)	Au | DNBA | $Ni(OH)_2$(ml)	Au | DNBA | $Ni(OH)_2$
Surface coverage (Γ)/mol cm^{-2}	9.1×10^{-9}	1.04×10^{-9}	3.1×10^{-8}
$E_{p,a}$/mV	345	350	340
$E_{p,c}$/mV	245	270	200
ΔE_p/mV	100	80	140
E^a_{fwhm}/mV	50	45	70
E^c_{fwhm}/mV	30	35	50

[a] Note: The voltammetric data are estimated from CVs recorded at 20 mV s^{-1} in 1 M KOH and the potential values are referred to MCE.

rates and ΔE_p increases with the scan rate [29]. In the case of electrodes modified with multilayers of $Ni(OH)_2$, the following behaviour [3,4] is observed usually. (i) Even at low scan rates, ΔE_p is greater than 60 mV, indicating relatively slow redox transformation and/or electron exchange process at the interface between the electrode substrate and $Ni^{2+/3+}$ redox centres. (ii) E^a_{fwhm} values are smaller than those expected (<90.6 mV) for surface-confined species which suggest attractive interactions between the redox sites in the film. (iii) Further, the anodic peaks are always higher and broader than the cathodic ones and they tend to be equal at low nickel hydroxide coverages. In Table 1 is presented a comparison of the voltammetric features observed for the Au \| $Ni(OH)_2$, Au \| DNBA \| $Ni(OH)_2$(ml) and Au \| DNBA \| $Ni(OH)_2$ electrodes. With Au \| DNBA \| $Ni(OH)_2$(ml) and Au \| DNBA \| $Ni(OH)_2$ electrodes, ΔE_p is greater than zero (cf. Table 1). This is in good agreement with high ΔE_p values noticed for the Au electrode modified directly (i.e. without a SAM intermediate layer) with $Ni(OH)_2$ (cf. Table 1) and also conforms to observations made earlier [3,4]. Further, E^a_{fwhm} values are smaller than the theoretically expected value of 90.6 mV [28] This possibly suggests the presence of attractive interactions among the surface species as noted earlier [3,4] with multilayered $Ni(OH)_2$ film on a bare Au surface. Moreover, from Table 1 it can be seen from the three different modified electrodes that the ΔE_p value increases as the thickness of the modified $Ni(OH)_2$ film increases. 'Whether the variation of film thickness influences the interactions among the adsorbate molecules and thereby contributes to the change in the ΔE_p values,' is not clear to us and needs independent investigations.

The above results reveal that on bare Au, overlayers of $Ni(OH)_2$ can be built to considerable thickness by electrochemical methods of modification [18,19]. By restricting the duration of modification on bare Au to only seven potential cycles, a film growth corresponding to about nine monolayers could be achieved. Prolonged potential cycling has yielded films of thickness approaching 100 monolayers. On the other hand, the modification on Au \| DNBA by the same procedure [18,19] has resulted in $Ni(OH)_2$ films, which attain a saturation growth corresponding to about 30 monolayers coverage. The reduction in film thickness observed in the presence of a DNBA SAM on the Au surface could be attributed to the slowing down of the electron transfer rate at the Au \| DNBA interface. Thus, the presence of a SAM of suitable organic molecules as an intermediate layer on the electrode surface enables immobilization of relatively very thin films of MO.

More importantly, the modification procedure described in this study, viz., treating the Au \| DNBA electrode in Ni^{2+} solution and then potentiodynamically cycling it in potassium ferricyanide and subsequently in KOH solutions, leads to the formation of a monolayer of $Ni(OH)_2$ film which is reported here for the first time. This achievement of a monolayer level $Ni(OH)_2$ modification could be understood in terms of the presence of the DNBA SAM as follows. The DNBA molecules, by virtue of Au-disulfide interactions, chemisorb strongly on the Au surface resulting in a near monolayer coverage. The –COOH groups of the DNBA molecules adsorbed on the electrode surface remain ionized in KCl solution (pH of the KCl solution is higher than the pK_a of DNBA) and chelate the Ni^{2+} ions from solution. Subsequently, during potential cycling in potassium ferricyanide solution it is derivatized to NiHCF and then to $Ni(OH)_2$ during cycling in KOH solution. The formation of surface-confined NiHCF moities during the first stage of modification becomes evident from the voltammetric

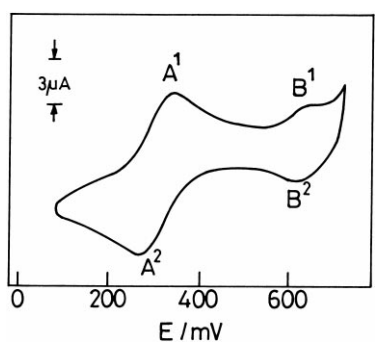

Fig. 5. CV recorded at the final stage of hexacyanoferrate modification of a Au \| DNBA electrode treated with Ni^{2+} solution, in 1 M KCl solution containing $K_3Fe(CN)_6$ (0.25 mM); sweep rate: 20 mV s^{-1}.

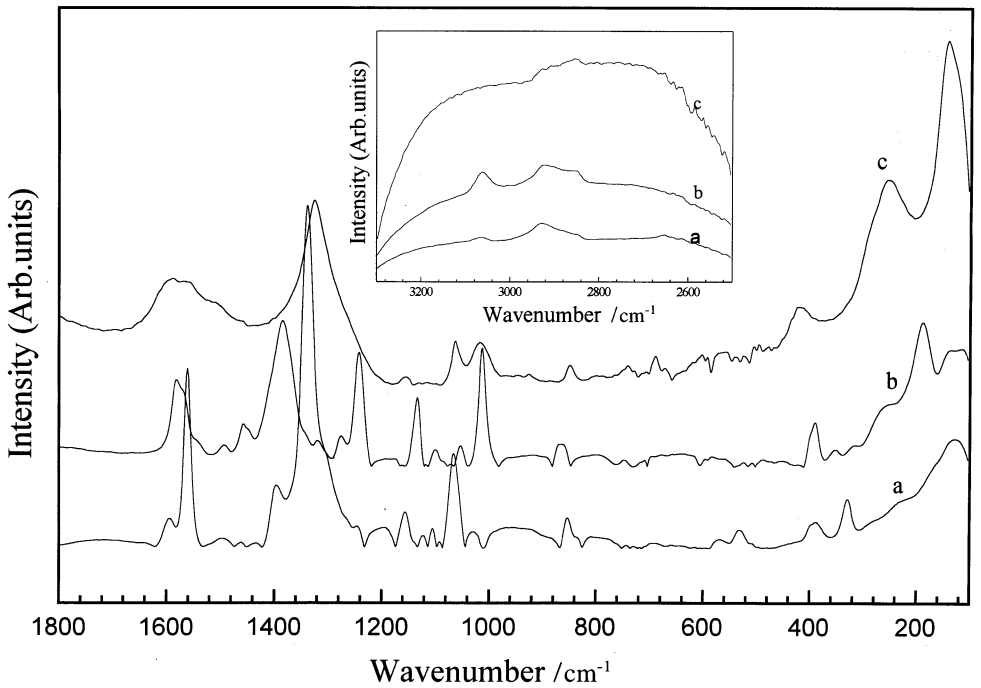

Fig. 6. SER spectra of (a) a bare DNBA monolayer on Au (b) after the first stage of reaction and (c) after the second stage of reaction. Inset shows the corresponding high frequency region.

features of the modified electrode shown in Fig. 5 The pair of peaks (B^1 and B^2) noticed at 0.634 and 0.604 V for the anodic and cathodic processes, respectively, and characterized by a ΔE_p value of 30 mV arise from the surface-confined NiHCF species [20] while the other pair of peaks (A^1 and A^2) with the ΔE_p value of 75 mV could be attributed to the redox behaviour of the solution species. Moreover, it is pertinent to note that this method of modification of the electrode surface yields NiHCF as an intermediate which upon cycling in KOH solution is converted to $Ni(OH)_2$ has also been confirmed earlier by XPS studies (cf. fig. 4 of Ref. [20]).

3.4. SERS and XPS characteristics of the modified electrodes.

In order to understand the electrode modification in its molecular detail, we performed SERS measurements of the DNBA coated electrodes. SERS active gold electrodes were prepared by electrochemical roughening [30]. To prepare roughened surfaces, linear potential sweep orcs were applied to Au electrodes in 0.1 M aqueous KCl solution. The initial potential was -0.20 V versus an $Ag \mid AgCl \mid KCl(sat)$ reference electrode, and the potential sweep was reversed at ca. $+1.20$ at a scan rate of 100 mV s^{-1}. The electrodes were removed from the solution at open circuit potential, washed with ethanol and then exposed to the DNBA solution. The electrode was mounted in the Raman spectrometer after repeated washing with absolute ethanol. SER spectra of the bare DNBA monolayer, the surface after reaction with $K_3Fe(CN)_6$ and after the $Ni(OH)_2$ film growth are shown in Fig. 6. The SER spectrum of the DNBA modified electrode can be understood in terms of the cleavage of the disulfide bond and the concomitant adsorption of the phenyl ring nearly parallel to the surface [31].

Frequencies of particular importance to this study are those due to the aromatic stretching mode at 3061 cm^{-1}, the phenyl ring deformation mode at 1586 cm^{-1} and the COO^- symmetric stretching mode at 1380 cm^{-1}. After the first stage of electrode modification, drastic changes are observed in the spectrum. The COO^- (sym.) mode at 1380 cm^{-1} increases in intensity, whereas the NO_2 (sym.) stretch at 1337 cm^{-1} is downshifted and reduced in intensity. One important feature noticed is the emergence of the band at 1005 cm^{-1} due to the ν_1 mode of the phenyl ring. The appearance of this band and a change in the COO^- (sym.) mode suggest a change in molecular geometry during the first stage of the reaction. It is important to note that during this stage of the reaction, the aromatic C–H stretching mode increases in intensity (see the inset of Fig. 6). The relative enhancement of certain vibrations of this kind could be attributed to the lifting up of the phenyl ring to a near perpendicular orientation. It is to be noted that such changes have been used to understand the changes in adsorbate geometry in a number of aromatic systems [32,33]. Although a lifting of the molecular plane could also be due to a change in the adsorbate

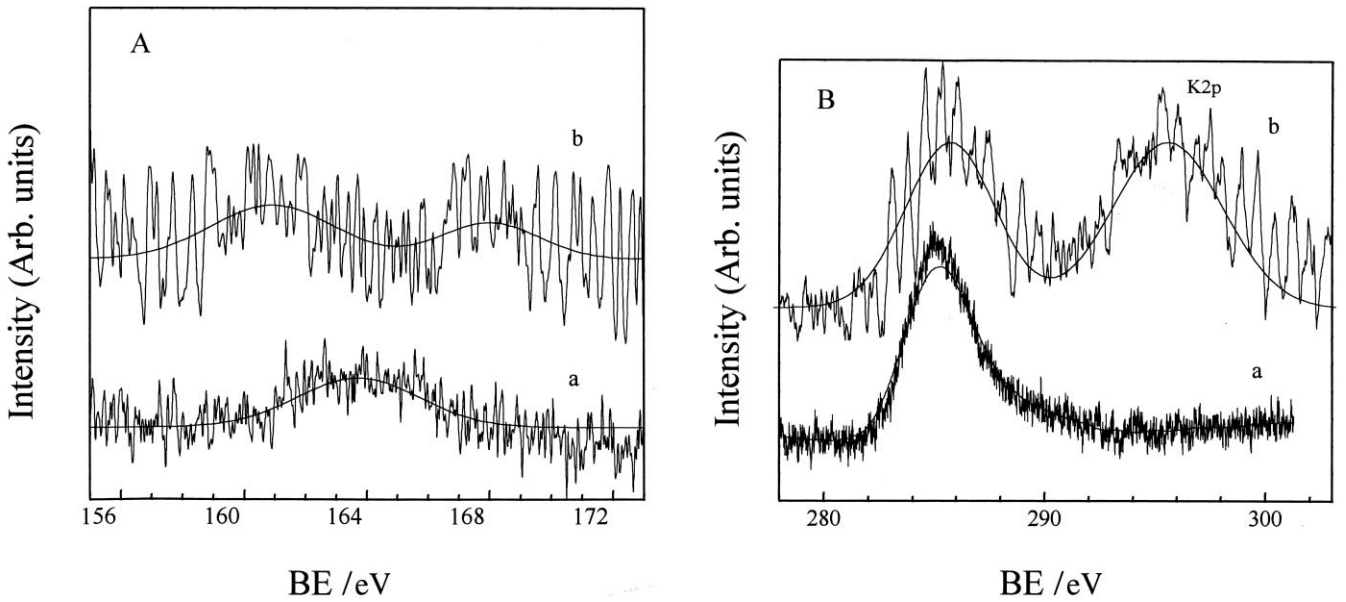

Fig. 7. XPS spectra in the (A) S2p region of the (a) unmodified and (b) modified DNBA monolayers. (B) C1s region of the (a) unmodified and (b) modified DNBA monolayers. (b) Shows also a K2p structure.

binding site from thiolate to carboxylate, we do not observe marked differences in the C–S region of the spectrum. Even in carboxyl-functionalized thiols, the adsorbate binding site is thiolate only and not carboxylate [34,35]. In view of the above, it may be concluded that the Ni-binding occurs with the carboxylate and not onto the sulfur. Upon the second stage of the reaction (containing the monolayer of $Ni(OH)_2$), many of the minor features of DNBA disappeared, although, the ring deformation mode and the COO^- (sym.) mode are prominently observed. Particularly important is the shift of the COO^- (sym.) mode to a lower frequency as a result of the suggested modification. This broad structure may also contain the NO_2 (sym.) stretch.

It may be recalled that $Ni(OH)_2$ shows distinct Raman frequencies at 479 and 560 cm^{-1} only when the sample is in the powder form [27]. Even for a thin film of about 2000 equivalent monolayers of $Ni(OH)_2$ no SERS signals were obtained [27]. Thus, the absence of SERS signals due to $Ni(OH)_2$ in Fig. 6 is not surprising. However, the observed changes in the spectral features in conjunction with the electrochemical data support the proposed chemical transformation. The retention of characteristic DNBA structures even after drastic electrochemical treatment points to the rigidity of the monolayer structure, which is again supported by the temperature dependent SERS investigation [31].

Changes in the elemental chemical structure were probed by XPS. In Fig. 7(A) we show the S2p region of the bare and modified monolayers. S2p of the unmodified SAM shows a composite structure, which could be understood on the basis of X-ray beam induced damage of thin monolayers [36,37]. Note that in the proposed adsorbate geometry, we assume that the phenyl ring is flat on the surface, which would increase the probability of surface damage due to X-ray exposure. Earlier investigations of dithiol monolayers have shown that the peaks observed are due to sulfonates or sulfates [36,37]. An important consequence of the reaction is the shifting of the peak to 162 eV, characteristic of the thiolate structure. The beam induced damaged product is observable at 168 eV, albeit at reduced intensity. In Fig. 7(B) we show the C1s region of the photoelectron spectrum of the bare DNBA monolayer and the monolayer after the second stage of modification. As a result of the chemical transformation K^+ is deposited in the monolayer as a remnant of the KOH

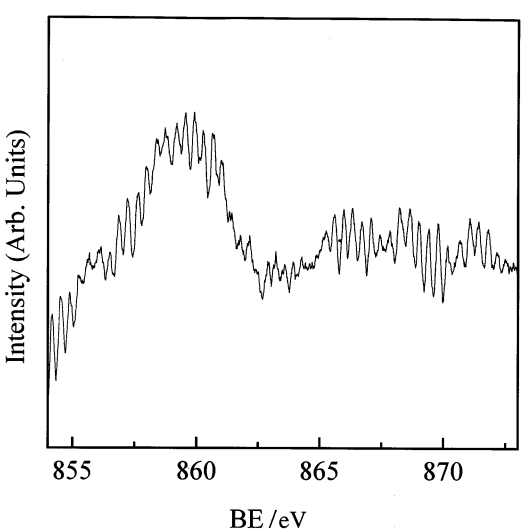

Fig. 8. XPS spectrum in the $Ni2p_{3/2}$ region of the modified DNBA.

cycling process. In Fig. 8 we give the Ni $2p_{3/2}$ region of the modified monolayer showing a characteristic BE structure attributed to Ni^{2+}. The N1s region of the unmodified DNBA shows a BE of 407 eV (not shown) attributed to NO_2 and a very similar BE is observed for the modified monolayer although this region is also composed of structures due to the KLL Auger structure of Ni. O1s in unmodified and modified monolayers occurs as a single peak at 532 eV BE.

SERS results in conjunction with XPS data suggest chemical modification of the monolayer. Retention of the SER spectrum of DNBA after modification and the preservation of S2p and N1s structures in XPS studies are clear indications of the presence of chemical modification of DNBA. The observation of the thiolate structure of the modified monolayer and the reduction in beam induced damage suggest the presence of a protective overlayer. The characteristic Ni2p BE attributed to Ni^{2+} again indicates the proposed modification. The lack of SER features of $Ni(OH)_2$ could be explained as due to the presence of this species as an overlayer on the DNBA monolayer. It is well known that SERS is particularly sensitive to the region close to the active surface and may well be insensitive to regions much above it [38].

3.5. Electrocatalysis of glucose

The catalytic nature of $Ni(OH)_2$ film obtained on Au | DNBA through modification is assessed by studying the electro-oxidation of glucose. Fig. 9 depicts the CVs recorded for the electro-oxidation of glucose (5 mM) in 1 M KOH at 20 mV s^{-1} on Au | DNBA | $Ni(OH)_2$(ml) (Fig. 9(a)) and Au | DNBA | $Ni(OH)_2$ (Fig. 9(b)) electrodes. The enhancement of the anodic peak at around 350 mV and the disappearance of the corresponding cathodic peak show that the glucose is electrocatalytically oxidized at the modified electrodes. For comparison, CVs recorded on bare Au and Au | DNBA electrodes for the electro-oxidation of glucose under the same experimental conditions are shown in Fig. 10

The catalytic oxidation of glucose is expected to follow the scheme below, involving the redox characteristics of the $Ni(OH)_2$ species

$$Ni(OH)_2 + OH^- \leftrightarrow NiOOH + H_2O + e^- \quad (1)$$

$$NiOOH + \text{glucose} \rightarrow Ni(OH)_2 + \text{products} \quad (2)$$

In all the three $Ni(OH)_2$-modified electrodes studied, catalytic oxidation of glucose is believed to follow the above reaction pathway.

It is known that the $Ni(OH)_2$ peak is followed immediately by the oxygen evolution reaction. Hence on the Au | $Ni(OH)_2$ electrode, the catalytic current due to glucose oxidation through the $Ni(OH)_2$ route is not well defined and could not be measured. On the Au | DNBA | $Ni(OH)_2$ electrode, the catalytic oxidation of glucose is well distinguished from the oxygen evolution current and could be estimated (indicated by an arrow in Fig. 9).

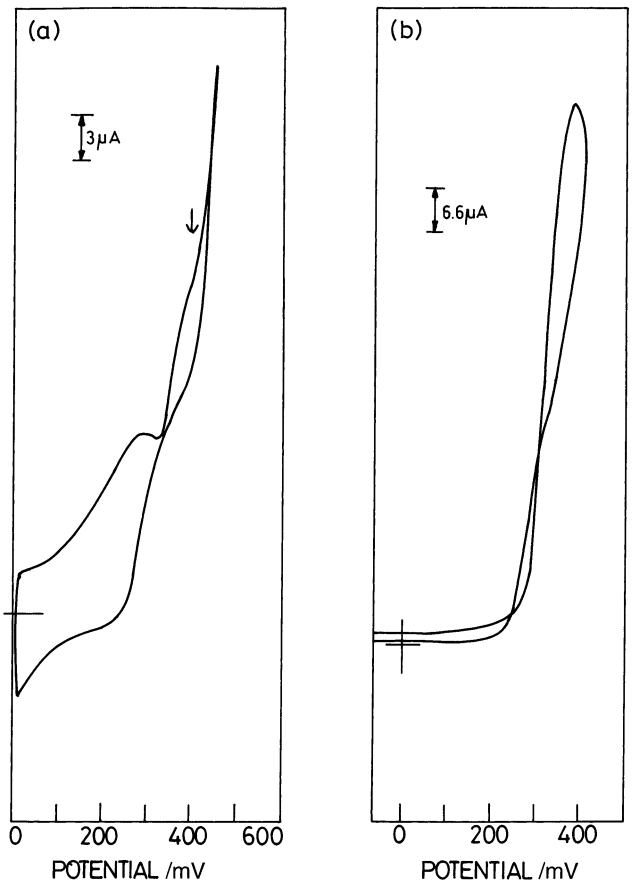

Fig. 9. CV response for the oxidation of glucose (5 mM) in 1 M KOH at 20 mV s^{-1} at (a) Au | DNBA | $Ni(OH)_2$(ml) and (b) Au | DNBA | $Ni(OH)_2$ electrodes.

At this point, it may be recalled that Pt [39,40] and Au [24] electrodes have earlier been reported as electrocatalysts for the oxidation of glucose. However, on Pt, it has also been observed that the electrode surface is extremely non-selective and susceptible to poisoning by irreversible adsorption of intermediates [40]. On the Au electrode, the interference due to adsorption of intermediates is considerably less when compared to Pt. On the other hand, the electrode has to be polarized to high potentials (i.e. 1.2 V vs. SCE) to ensure the presence of gold oxide species which catalyses the glucose oxidation [24].

The present investigations reveal that the glucose oxidation is electrocatalysed by $Ni(OH)_2$ species immobilized on the Au | DNBA electrode. The electrocatalytic effect of surface-confined $Ni(OH)_2$ species on

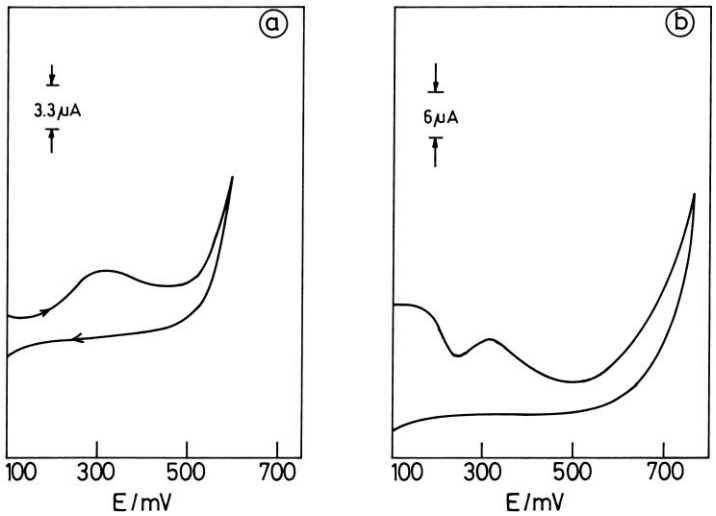

Fig. 10. CV for the electro-oxidation of glucose (5 mM) in 1 M KOH at 20 mV s^{-1} on (a) bare Au and (b) Au | DNBA electrodes.

the oxidation of polyhydric alcohols and sugars has already been reported [2]. Efficacy of the above species in catalyzing glucose oxidation also has been shown by immobilizing $Ni(OH)_2$ overlayers on a glassy carbon surface [19]. The results of present investigations are in conformity with the above.

4. Conclusions

These investigations have opened up the possibility of preparing very thin films of oxide/hydroxide catalysts using the self-assembly approach. The SAM formed from molecules having suitable terminal functional groups can chelate/bond with catalyst species. The presence of SAMs as intermediate layers helps in growing very thin films of metal oxides since formation of thick films is invariably prevented from the saturation of film growth achieved in a few cycles during the preparation. Employing a SAM of 5,5′-dithiobis(2-nitrobenzoic acid) as the intermediate layer, nickel hydroxide films varying in thickness from a single monolayer to more than a hundred monolayers were formed on gold electrodes. Formation of a single monolayer of nickel hydroxide on the electrode surface by the electrochemical modification reported here is believed to be the first of its kind. The voltammetric investigations on the oxidation of glucose at the modified electrodes have shown that the oxidation proceeds through the surface-confined, catalytic $Ni(OH)_2$ species.

Acknowledgements

The ‘Spectroscopic characterization’ and ‘glass blowing’ sections of the Institute are thanked for their help in collecting the UV-vis spectral data and designing the electrochemical cell respectively. TP thanks the Department of Science and Technology, Government of India, Rajiv Gandhi Foundation and the Jawaharlal Nehru Centre for Advanced Research for supporting his research program on SAMs. NS thanks the Council of Scientific and Industrial Research, New Delhi, for a research fellowship.

References

[1] V.E. Henrich, Progr. Surf. Sci. 50 (1993) 77.
[2] I.G. Casella, T.R.I. Cataldi, A.M. Salvi, E. Desimoni, Anal. Chem. 65 (1993) 3143.
[3] T.R.I. Cataldi, D. Centonze, G. Ricciardi, Electroanalysis 7 (1995) 312.
[4] T.R.I. Cataldi, E. Desimoni, G. Ricciardi, F. Lelj, Electroanalysis 7 (1995) 435.
[5] C.M. Lampert, Sol. Energy Mater. 11 (1984) 1.
[6] C.M. Lampert, T.R. Omstead, P.C. Yu, Sol. Energy Mater. 14 (1986) 161.
[7] C.M. Lampert, G. Nazri, P.C. Yu, Sol. Energy Mater. 16 (1987) 1.
[8] L.D. Burke, M.E. Lyons, O.J. Murphy, J. Electroanal. Chem. 132 (1982) 247.
[9] D.R. Jung, A.W. Czanderna, Crit. Rev. Solid-State Mater. Sci. 19 (1) (1994) 1.
[10] I. Rubinstein, S. Steinberg, Y. Tor, A. Shanzer, J. Sagiv, Nature 332 (1988) 426.
[11] I. Turyan, D. Mandler, Anal. Chem. 69 (1997) 894.
[12] S. Bharathi, V. Yegnaraman, G. Prabhakara Rao, Langmuir 11 (1995) 666.
[13] I. Turyan, D. Mandler, Anal. Chem. 66 (1994) 58.
[14] G.W. Briggs, E. Jones, W.F.K. Wynes-Jones, Trans. Faraday. Soc. 51 (1995) 1433.
[15] G.W. Briggs, Special Periodical Report, Electrochemistry, vol. 4, The Chemical Society, London, 1974, p. 33.
[16] S. Dong, J. Li, Bioelectrochem. Bioenerg. 42 (1997) 7.
[17] K. Gleira, H.A.O. Hill, J.A. Chambers, J. Electroanal. Chem. 267 (1989) 83.

[18] J. James, H. Gomathi, G. Prabhakara Rao, Electrochim. Acta 36 (1991) 1537.
[19] S. Berchmans, H. Gomathi, G. Prabhakara Rao, J. Electroanal. Chem. 394 (1995) 267.
[20] T.R.I. Cataldi, R. Guascito, A.M. Salvi, J. Electroanal. Chem. 417 (1996) 83.
[21] R.S. Nicholson, Anal. Chem. 37 (1965) 1351.
[22] K.T. Kinnear, H.G. Monbonquette, Anal. Chem. 6 (1997) 1771.
[23] D.R. Lide (Ed.), CRC Handbook of Chemistry and Physics, 74th edition, CRC Press, Boca Raton, 1993, p. 8.45.
[24] E.B. Makovos, C.C. Liu, Bioelectrochem. Bioenerg. 15 (1986) 157.
[25] A.B. Bocarsly, S.A. Galvin, S. Sinha, J. Electroanal. Chem. 130 (1983) 1319.
[26] R.S. Schreber Guzman, J.R. Vilche, A.J. Arvia, J. Electrochem. Soc. 125 (1978) 1578.
[27] J. Desilvestro, D.A. Corrigan, M.J. Weaver, J. Electrochem. Soc. 135 (1988) 885.
[28] R.W. Murray, in: A.J. Bard (Ed.), Electroanalytical Chemistry, Chapter 3, vol. 13, Marcel Dekker, New York, 1984.
[29] C.P. Andrieux, J.M. Saveant, J. Electroanal. Chem. 111 (1980) 377.
[30] M.A. Bryant, J.E. Pemberton, J. Am. Chem. Soc 113 (1991) 8284.
[31] N. Sandhyarani, K.V.G.K. Murty, S. Berchmans, V. Yegnaraman, T. Pradeep. SER spectrum of DNBA and its assignment, to be published.
[32] P. Gao, M.J. Weaver, J. Phys. Chem. 89 (1985) 5040.
[33] X. Gao, J.P. Davies, M.J. Weaver, J. Phys. Chem. 94 (1990) 6858.
[34] R.V. Duevel, R.M. Corn, Anal. Chem. 64 (1992) 337.
[35] Q. Cheng, A. Brajter-Toth, Anal. Chem. 64 (1992) 1998.
[36] V.L. Colvin, A.N. Goldstein, A.P. Alivisatos, J. Am. Chem. Soc. 114 (1992) 5221.
[37] K.V.G.K. Murty, M. Venkataramanan, T Pradeep, Langmuir, in press.
[38] W. Suetaka, Surface Infrared and Raman Spectroscopy, Methods and Applications, Plenum Press, New York, 1995.
[39] H.-W. Lei, B. Wu, C.-S. Cha, H. Kita, J. Electroanal. Chem. 382 (1995) 103.
[40] C.P. Wilde, M. Zhang, J. Electroanal. Chem. 340 (1992) 241.